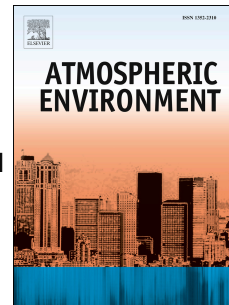


Accepted Manuscript

Modelled Atmospheric Contribution to Nitrogen Eutrophication in the English Channel and the Southern North Sea

G. Djambazov , K. Pericleous



PII: S1352-2310(14)00950-9

DOI: [10.1016/j.atmosenv.2014.11.071](https://doi.org/10.1016/j.atmosenv.2014.11.071)

Reference: AEA 13452

To appear in: *Atmospheric Environment*

Received Date: 14 July 2014

Revised Date: 21 November 2014

Accepted Date: 23 November 2014

Please cite this article as: Djambazov, G., Pericleous, K., Modelled Atmospheric Contribution to Nitrogen Eutrophication in the English Channel and the Southern North Sea, *Atmospheric Environment* (2015), doi: 10.1016/j.atmosenv.2014.11.071.

This is a PDF file of an unedited manuscript that has been accepted for publication. As a service to our customers we are providing this early version of the manuscript. The manuscript will undergo copyediting, typesetting, and review of the resulting proof before it is published in its final form. Please note that during the production process errors may be discovered which could affect the content, and all legal disclaimers that apply to the journal pertain.

1 Modelled Atmospheric Contribution to Nitrogen Eutrophication in the English Channel 2 and the Southern North Sea

3
4 G. Djambazov^{1*}, K. Pericleous¹

5
6 ¹Centre for Numerical Modelling and Process Analysis
7 University of Greenwich
8

9 Abstract

10
11 Eutrophication of the coastal waters results in algal blooms which may be harmful to the
12 marine ecosystem and coastal economy. The main sources of nutrients are the rivers but an
13 unquantified amount of nitrogen is also transported from ground sources via the atmosphere
14 and deposited to the sea directly by rain and turbulent diffusion. A Lagrangian Particle
15 Dispersion (LPD) model based on the open source code FLEXPART (<http://flexpart.eu>) is
16 described that quantifies the dissolved nitrogen coming from the air in the English Channel
17 and Southern North Sea (the '2Seas' geographical region). The model uses meteorological
18 records, emissions data and LPD computations to simulate the motion and deposition of
19 nitrogen compounds. The emission sources contributing to the deposition are individually
20 identified, and calculated concentrations are compared with ground measurements in selected
21 locations. The highest calculated atmospheric depositions to the sea in the considered region
22 are found to be along the Belgium-Netherlands coast.
23

24 **Keywords:** atmospheric transport; pollutants; eutrophication; Lagrangian particle dispersion
25

26 1. Introduction

27
28 Nutrient enrichment of estuaries and coastal waters by human activities causes phytoplankton
29 and algae to grow more than it would do otherwise (e.g. Peierls, 1991; Anderson, 2002).
30 Provided adequate light is available, phosphorus and nitrogen are the nutrients that limit
31 phytoplankton growth in aquatic systems, and primary production in estuaries and coastal
32 waters is thought to be limited by nitrogen availability (Anderson, 2002). In contrast,
33 freshwater phytoplankton tends to be limited by phosphorus availability, although the extent
34 and severity of nitrogen limitation remains open to question (Hecky, 1988; Boynton, 1982;
35 Nedwell, 2002) and in situations where light penetration is poor as in turbid estuarine and
36 coastal waters, even high nutrient concentrations may not lead to significant algal growth. As
37 a societal problem, eutrophication and consequent algal overgrowth has several undesirable
38 socioeconomic and environmental consequences. The additional growth does not enter the
39 marine food chain and by decaying depletes the water of oxygen and thus causes harm to
40 marine life. Another side effect of the decay is unsightly foam on the beaches, which affects
41 tourism and dependant commercial activities.
42

43 Groundwater transport constitutes the main source of eutrophicants and therefore the main
44 target of regulative corrective measures (Anderson, 2002). Nevertheless, atmospheric
45 deposition is also significant adding from 300 to 1000 mg Nm⁻² yr⁻¹ to coastal waters in
46 biologically active forms NO_x, NH₃/NH₄⁺, and in dissolved organic nitrogen (Paerl, 1997).
47 Atmospheric tracer-based model results show that atmospheric deposition accounts for 6% of
48 the external nitrogen inputs in the North Sea (Troost, 2013). This percentage however is
49 shown to vary strongly with region. For example, in the OSPAR area NL-O2 (OSPAR,
50 2013), 16% of the total nitrogen originates from atmospheric deposition. Furthermore, model

* Corresponding author. Tel.: +442083319589
E-mail address: G.Djambazov@gre.ac.uk

51 results show that primary production rates are disproportionately affected by atmospheric
 52 deposition, possibly due to a change in the carbon-to-nitrogen ratio (Troost, 2013). Budgeting
 53 approaches (Spokes, 2005) suggest that the atmosphere can in some situations provide
 54 enough nitrogen to produce a large increase in phytoplankton growth. The modelled regional
 55 and temporal variation reflects the highly episodic nature of atmospheric deposition and the
 56 strong gradients away from source regions.

57
 58 A parallel study in the Baltic Sea shows that atmospheric deposition, primarily from burning
 59 fossil fuels (land based and shipping), accounts for 25 % of nitrogen input (WRI, 2014). Even
 60 more significant atmospheric contributions were found in Chesapeake Bay, U.S (up to 30%
 61 of all nitrogen inputs) and in some other areas in the U.S. North Atlantic, where atmospheric
 62 deposition of nitrogen can exceed riverine nitrogen inputs to coastal areas (Spokes, 2005). It
 63 is evident from these observations, that the atmospheric contribution is an essential part of
 64 any inventory of nutrients leading to algal growth.

65
 66 As stated above, the nutrients phytoplankton species need are inorganic compounds of
 67 nitrogen, phosphorus and silicon. Of these only nitrogen-bearing compounds such as
 68 nitrogen oxides and ammonia, being gases, can be airborne in significant quantities. While in
 69 some cases of blooming phytoplankton the availability of phosphorus may be the growth-
 70 limiting factor (Ly, 2014), nitrogen may still play a part for some species. So a model of the
 71 atmospheric input of eutrophicants is a valuable tool in the study, prediction and prevention
 72 of harmful algal blooms.

73
 74 This paper is an illustration of how the three main components of such a model – weather
 75 data, emissions data and computer simulations – can be combined into a working tool for
 76 quantitative estimates of the atmospheric inputs.

77 78 **2. Lagrangian Transport Computer Model**

79
 80 Emitted nitrogen-containing gases are carried and dispersed by the wind before being
 81 deposited to the ground or sea. A publically available, open source software package
 82 FLEXPART (Stohl, 2005) implementing the Lagrangian Particle Dispersion method is used in
 83 this study. It can simulate the movement of pollutants in the atmosphere and includes also
 84 algorithms for determining the rates of their deposition onto various surfaces (e.g. Plainiotis
 85 2005a, 2005b, 2010). In the model, each of the traced ‘particles’ is assumed to be carrying a
 86 certain quantity of the investigated substance. Concentrations are calculated after dispersion
 87 by atmospheric turbulence is taken into account. From the concentrations, using specific
 88 deposition properties of each traced gas, deposited quantities are calculated on a user-
 89 prescribed grid.

90 91 *2.1 FLEXPART Equations*

92 93 2.1.1 Particle trajectory calculations

94
 95 The trajectory equation (Stohl, 1998)

$$\frac{d\mathbf{X}}{dt} = \mathbf{v}[\mathbf{X}(t)]$$

96 with \mathbf{X} the position vector, \mathbf{v} the particle velocity, t the time and Δt the time step is integrated
 97 using the “zero acceleration” scheme

$$\mathbf{X}(t + \Delta t) = \mathbf{X}(t) + \mathbf{v}(\mathbf{X}, t)\Delta t.$$

98 The wind vector $\mathbf{v} = \bar{\mathbf{v}} + \mathbf{v}_t + \mathbf{v}_m$ is composed of the grid-scale wind \mathbf{v} , the turbulent wind
 99 fluctuations \mathbf{v}_t and the mesoscale wind fluctuations \mathbf{v}_m (Stohl, 2005).

100

101 Turbulent motions are represented assuming a Markov process based on the Langevin
 102 equation (Thomson, 1987) for each turbulent wind component v_{t_i} , $i = 1 \dots 3$. The
 103 formulation includes a drift term and a diffusion term which are functions of the position, the
 104 turbulent velocity and time. Cross-correlations between the different turbulent wind
 105 components are not taken into account, since they have little effect for long-range dispersion
 106 (Uliasz, 1994).

107

108 Mesoscale motions (sub-grid motions which are not turbulent in nature) need to be taken into
 109 account since they can accelerate the growth of a dispersing plume. Updrafts in convective
 110 clouds that occur in conjunction with downdrafts within the clouds and compensating
 111 subsidence in the cloud-free surroundings are modelled by a convective parameterization
 112 scheme.

113

114 2.1.2 Wet deposition

115

116 Based on the humidity and temperature from the meteorological input data, the occurrence of
 117 clouds is calculated. After that separately in-cloud and below-cloud ‘scavenging’ of the
 118 transported substances are computed in the form of an exponential decay process for the
 119 particle mass m :

$$120 \quad m(t + \Delta t) = m(t)e^{-\Lambda \Delta t}.$$

121 For gases the *in-cloud* scavenging coefficient Λ [s^{-1}] is

$$\Lambda = \frac{I}{H c_{eff}}$$

122 where I [mm/h] is the precipitation rate, H is the height over which scavenging takes place
 123 and c_{eff} is effective cloud liquid water content.

124

125 The *below-cloud* scavenging coefficient is $\Lambda = AI^B$ where both A and B are empirical
 126 parameters specific for each modelled gas. Sub-grid variability of the precipitation is also
 127 taken into account for the wet deposition via the meteorological data for ‘total cloud cover’,
 128 ‘large scale precipitation’ and ‘convective precipitation’ (Stohl, 2005).

129

130 2.1.3 Dry deposition

131

132 The downward flux due to dry deposition F_C of a species with concentration C at height z is
 133 described by a deposition velocity

$$134 \quad v_d(z) = -F_C/C(z).$$

135 For *gases* the deposition velocity is represented as the inverse of the sum of the following
 136 ‘resistances’

$$|v_d(z)| = [r_a(z) + r_b + r_c]^{-1}$$

137 where r_a is the aerodynamic resistance between z and the surface, r_b is the quasilaminar
 138 sublayer resistance, and r_c is the bulk surface resistance. These are calculated from the
 139 atmospheric boundary layer properties contained in the meteorological input data and from
 140 the land-use surface data within FLEXPART.

141

142

143

144 2.2 Required input data

145

146 The FLEXPART algorithm needs 3-dimensional, time-dependent meteorological and
147 emissions data as input for the investigated geographical region and time period. The
148 weather data include wind velocities, humidity, temperature, pressure, sunshine, precipitation
149 and turbulence in the atmospheric boundary layer. The emissions inputs are in the form of a
150 list of 4-dimensional space-time 'boxes' corresponding to the grid cells on which the
151 emissions data are available.

152

153 3. Weather Data

154

155 Past records of the main meteorological variables for the whole world or for a chosen region
156 can be obtained free of charge from at least two sites: the US National Centers for
157 Environmental Prediction (NCEP, 2014) and the European Centre for Medium-Range
158 Weather Forecasts (ECMWF, 2014). Since this work is sponsored by a European project
159 (ISECA, 2014), preference was given to the latter, also because FLEXPART contains a direct
160 interface to the ECMWF data. The recommended frequency of weather records for best
161 accuracy in FLEXPART is one every 3 hours; however both analyses are available in 6-hour
162 periods and, bearing in mind that the eutrophication simulations should cover many weeks
163 and months, the 6-hour interval was assumed.

164 The best spatial resolution for publicly available weather records is on a regular grid with
165 0.75 degree spacing in the ERA-Interim reanalysis (ECMWF, 2014). Vertically, the
166 resolution of this dataset is 60 levels covering the troposphere and the lower stratosphere
167 where atmospheric transport occurs. Choosing a suitable domain covering Western Europe
168 helps keep these data files to a manageable size (about 2 megabytes, unzipped, for each 3D
169 record). Avoiding too wide a region means less downloading time for the weather data. The
170 selected geographical area contains the English Channel and the southern part of the North
171 Sea which is the object of the present study and includes the surrounding land masses, i.e. the
172 '2Seas' Region (INTERREG, 2014). Bearing in mind that nitrogen oxides will be one of the
173 main species whose transport needs to be modelled, the domain is extended eastwards to
174 include the heavily industrialised western Germany (12° E). A similar span is chosen to the
175 west of the Dover Straights (9° W) and the south and north boundaries are chosen to include
176 most of France and Britain (44° N to 57° N). All the data are in binary format and a
177 decoding software package (GRIB_API) is freely and publicly available from ECMWF for
178 use in FLEXPART (e.g. Plainiotis, 2010).

179

180 Full three-dimensional values are obtained for temperature, eastward and northward wind
181 velocity components, vertical velocity and humidity. Two-dimensional (surface) data are
182 needed for atmospheric pressure, terrain height, solar radiation, cloud cover, precipitation,
183 heat flux, horizontal components of turbulent stress and dew-point temperature. The three-
184 dimensional variables were downloaded in three groups (due to server file size limitations),
185 one month worth of data at a time, and the 2D surface variables appear in two other groups
186 (analysis and 12-hour forecasts, for some accumulated variables) also in monthly files.
187 Decoding, de-accumulation (of precipitation and boundary turbulence data) and regrouping
188 were carried out to form the 6-hourly records needed by FLEXPART. Figure 1 illustrates the
189 vertical and temporal (during one month) profile of the wind data at one point of the grid
190 located in the English Channel. In total, two full years (2009 and 2011) of meteorological
191 records were downloaded and pre-processed for use with FLEXPART. Refinement of the
192 horizontal resolution of the weather data was tested with the publicly available software

193 package (WRF, 2014) but this was considered unnecessary for eutrophication studies and is
 194 not presented here.

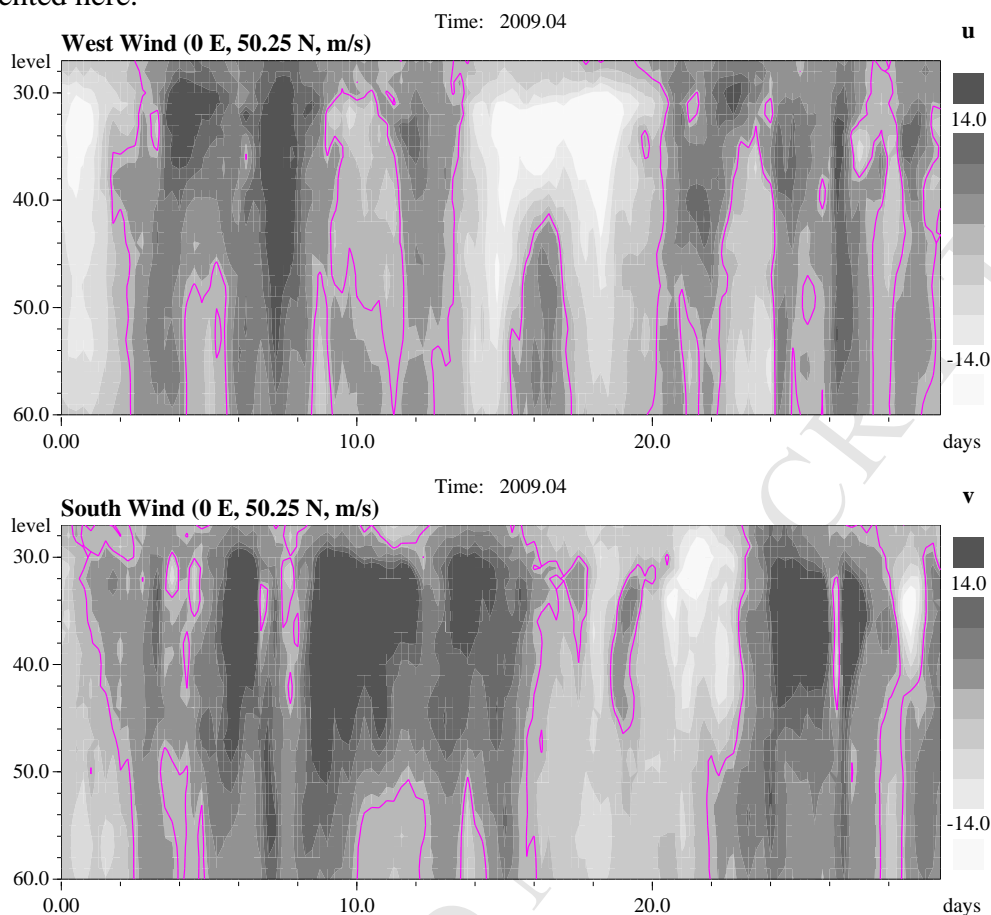


Figure 1. Wind components (u – eastward, v – northward) sample vertical record in April 2009 for 0°E, 50.25°W. The strongest winds at around model level 37 form the jet stream; level 60 is the ground.

195

196

197 4. Emissions

198

199 4.1 *Coarse-Grid EMEP Data*

200

201 The European Monitoring and Evaluation Programme (EMEP) maintain a website (WebDab,
 202 2014) with *freely* available gridded emissions data for the main air pollutants including
 203 nitrogen oxides and ammonia. Yearly emitted quantities (Figure 2) are currently offered on a
 204 50 km by 50km grid (EMEP, 2014) and a new fine grid with 0.1 degree resolution (CEIP,
 205 2015) is planned from 2015 onwards. The data are compiled from the yearly reports of the
 206 participating countries and can be very useful for atmospheric transport eutrophication
 207 modelling. One can see in Figure 2 that the highest nitrogen oxides emissions are around
 208 cities and industrial areas while the highest ammonia emissions are in agricultural areas. In
 209 this study proprietary fine-grid data were available (see next subsection) and they were used
 210 in place of the EMEP emissions.

211

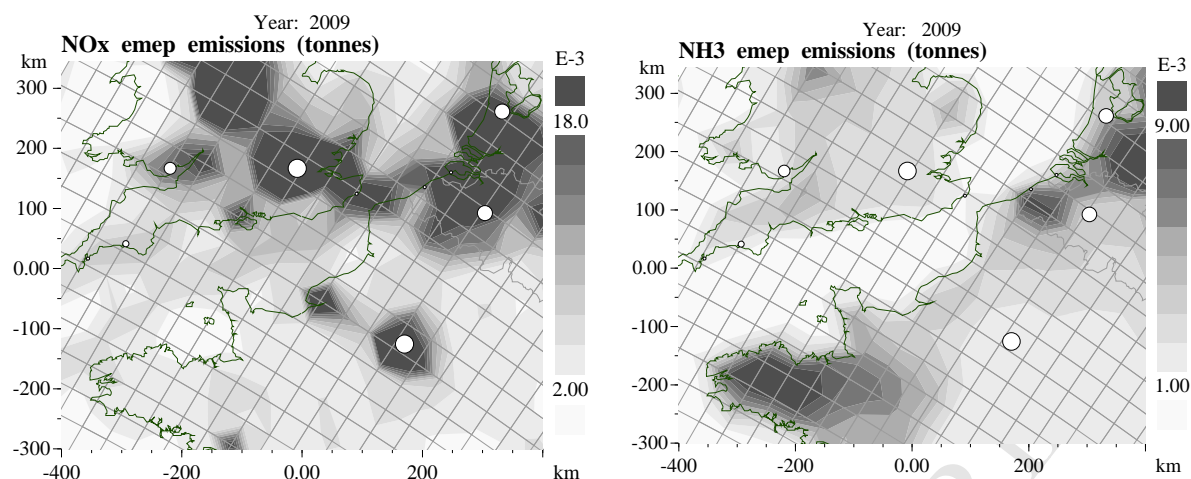


Figure 2. Emission of nitrogen oxides (left) and ammonia (right) as used in EMEP models (tonnes/year) in 2009. The white circles here and below show the cities of Cardiff, London, Paris, Brussels and Amsterdam.

212

213

4.2 *Fine Grid*

214

215 As part of the (ISECA, 2014) project, one of the partners - the Flemish Institute for
 216 Technological Research (VITO) – provided its refined database to be included in the
 217 simulations whose results are presented here. The fine grid of this database is 7x7 km.
 218 Emissions time profiles were also provided representing the daily, weekly and seasonal
 219 cycles. The fine-gridded data are derived from the country-reported totals and from
 220 information about what is where on the ground using a unique algorithm (Maes et al., 2009).
 221 In order to highlight the local contribution to local eutrophication, only sources within the
 222 ISECA target region (-6 to 7°E, 48 to 54°N) are included in the simulations. The emitted
 223 quantities are classified in the database in categories (SNAP sectors) according to the
 224 Standard Nomenclature for Atmospheric Pollutants (SNAP, 2014). Figure 3 shows the
 225 overall quantities emitted in the ISECA region for each sector for the years selected in the
 226 database.

227

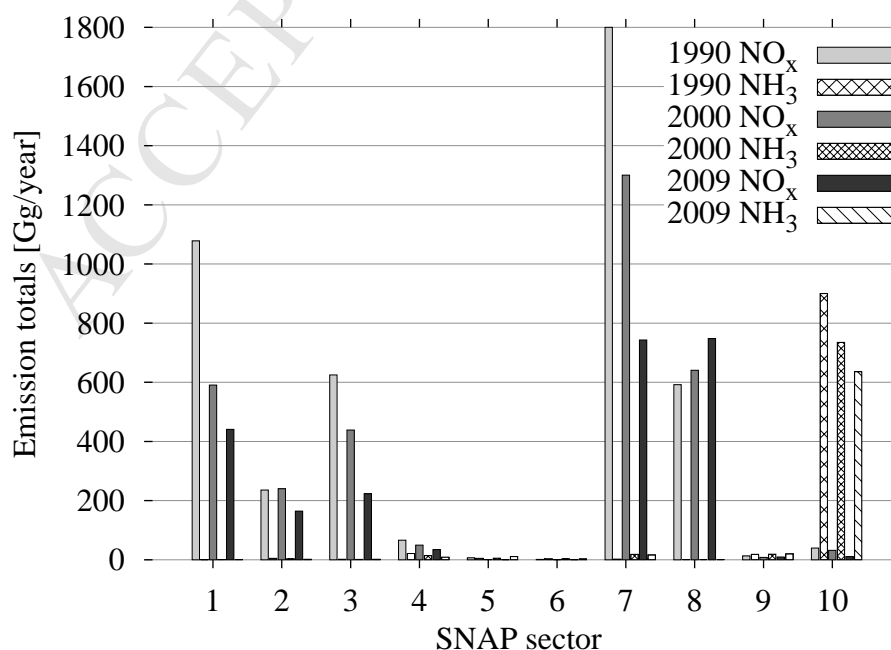


Figure 3. Fine grid emissions totals (Gg/year) for each Standard Nomenclature for Atmospheric Pollutants (SNAP) sector in the ISECA target region for representative years 1990, 2000 and 2009

228

229 It can be seen the main contributors in this geographical region are ‘Combustion in energy
230 and transformation industries’ (SNAP sector 1), ‘Non-industrial combustion plants’ (SNAP
231 sector 2), ‘Combustion in manufacturing industry’ (SNAP sector 3), ‘Road transport’ (SNAP
232 sector 7), ‘Other mobile sources and machinery’ (SNAP sector 8) and ‘Agriculture’ for
233 ammonia (SNAP sector 10). These are the data sources used to obtain the results presented
234 in Section 6. Most nitrogen oxides and ammonia emissions exhibit downward trends over the
235 years; the only exception is SNAP sector 8 which includes shipping through the Dover
236 Straights which is on the increase.

237

238 5. Model Validation

239

240 The concentrations calculated by FLEXPART at a number of prescribed receptor points on the
241 ground can be used to check the simulation results against available measurements.

242 The publicly available European Air Quality Database (AirBase, 2014) maintained by the
243 European Environment Agency was used to obtain measurement data for nitrogen oxides
244 concentrations from selected observation sites for the year 2009. (That is the latest year for
245 which fine-grid emissions data were available within the ISECA project.) A denser network
246 of measuring stations (KentAir, 2014) at various locations in Kent, UK also offers free data
247 for that region but AirBase was chosen for the validation because it includes stations from
248 different countries under the same format. Out of the many monitoring stations in the
249 dataset, a few suburban and rural sites (located near the coast in the target region) were
250 selected (Table 1) because the others, indicated in the database as being situated by roads,
251 would show local variations that are not represented in the model.

252

253 **Table 1.** Monitoring stations and model statistics

Station Code	Town/Place	Pollutant	Station Type	East deg	North deg	Height m	RMSE, normalised	Bias, normalised	Correl. coeff.
BETN012	Moerkerke	NO _x	suburban	3.36	51.26	3	0.68	-0.26	0.79
BETN029	Veurne	NO _x	rural	2.58	51.02	2	0.76	-0.31	0.72
FR10007	St. Pol-Mer	NO ₂	suburban	2.34	51.03	3	1.06	0.78	0.77
FR10012	Mardyck	NO ₂	industrial	2.25	51.02	4	1.1	0.77	0.67
FR10025	Sangatte	NO ₂	suburban	1.77	50.95	2	0.99	0.33	0.64
FR10029	Cappelle	NO ₂	urban	2.36	51.00	2	1.13	0.88	0.77
FR10032	Outreau	NO ₂	suburban	1.58	50.69	54	0.72	-0.14	0.76
GB0038R	Lullington	NO _x	rural	0.18	50.79	125	1.03	0.12	0.61
GB0617A	Rochester	NO _x	rural	0.63	51.46	14	1.27	0.70	0.71
GB0737A	Canterbury	NO _x	urban	1.10	51.27	35	0.84	-0.36	0.66
NL00235	Huijbergen	NO _x	rural	4.36	51.44	18	0.77	-0.04	0.64
NL00301	Zierikzee	NO _x	rural	3.92	51.64	-1	0.63	-0.19	0.83
NL00437	Westmaas	NO _x	rural	4.45	51.79	-1	0.62	-0.18	0.81

254

255 The statistical quantities indicating the modelling quality (Thunis, 2012) for the whole of
256 2009 and shown in Table 1 for comparison of the model calculations with station
257 measurements are the following: *RMSE, normalised* – root mean square error divided by the
258 standard deviation (SD) of the observations; *Bias, normalised* – mean bias of the model
259 divided by observations SD; *Corel. coeff.* – Pearson correlation coefficient of daily model
260 results and measured data. The model calculations are for total nitrogen oxides (NO_x)

261 expressed as NO_2 . However the French stations in the table report only the concentrations of
262 NO_2 , hence the positive bias of the model results.

263
264 It should be noted, that the model does not include far-away sources. For example, if
265 nitrogen oxides emitted to the west of the 2Seas target region are carried by the wind and
266 some atmospheric process (e.g. rain) causes the deposition of substantial amounts within the
267 region, this will not be picked up by the current model. This explains the predominantly
268 negative bias for stations reporting NO_x .

269

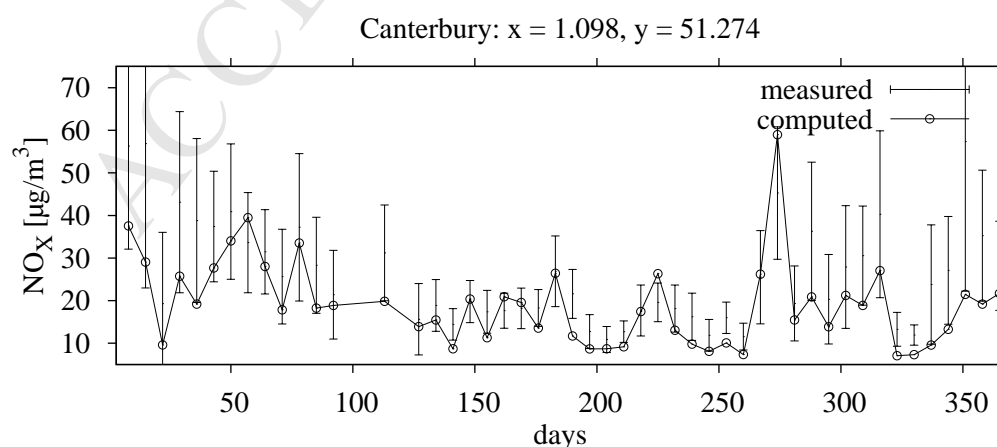
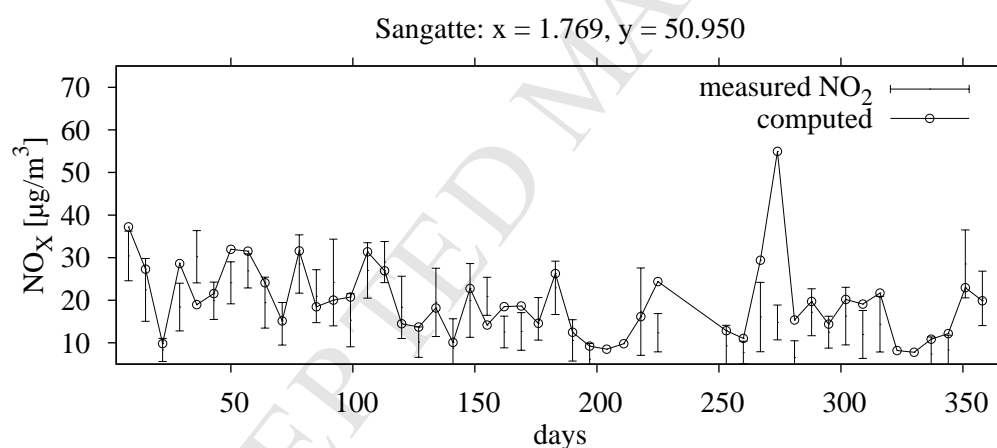
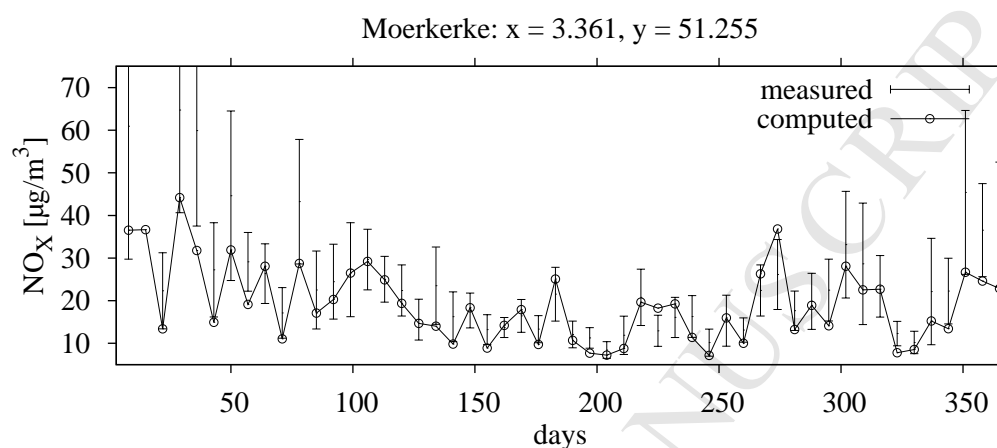


Figure 4. Validation comparisons between modelled and measured concentrations of nitrogen oxides (weekly averages at selected stations) in 2009

270

271 The comparison in Figure 4 shows weekly concentration averages of nitrogen oxides (as
 272 NO_2 , in micrograms per cubic metre) at some of the monitoring stations from Table 1. The
 273 error-bars of the measured quantities represent the standard deviation of the observations
 274 calculated within each weekly average from the reported hourly measurements. The
 275 corresponding calculated values are the means of 7 daily results output by Flexpart which are
 276 themselves daily concentration averages.

277

278 The graphs (Figure 4) and the correlations (Table 1) show that the computed results generally
 279 exhibit the right trends and are in the right range of values. Overall, the model accuracy is
 280 acceptable for the stated purpose of showing the contribution of the local sources to the
 281 eutrophication in the chosen target region.

282

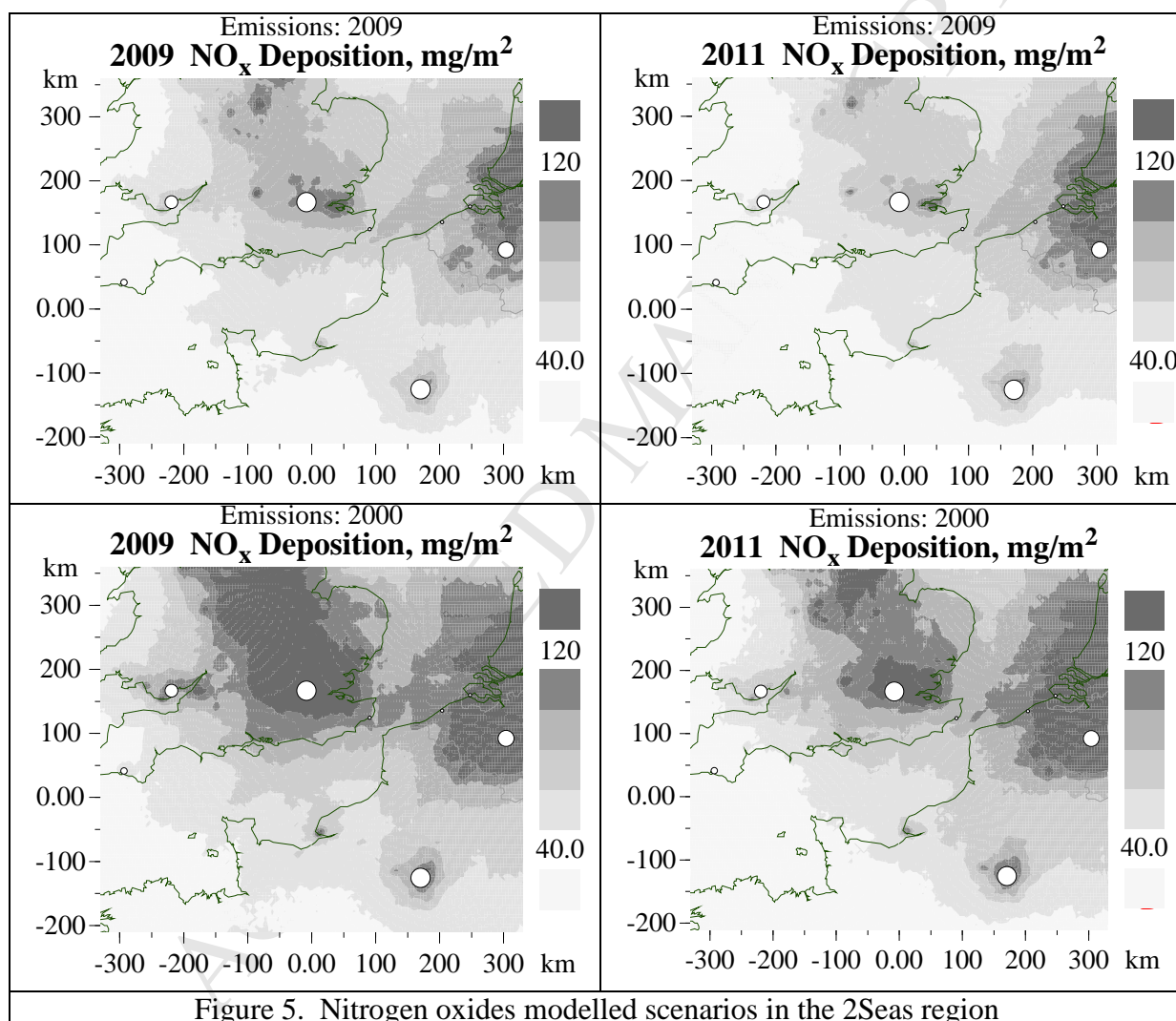


Figure 5. Nitrogen oxides modelled scenarios in the 2Seas region

283

284 6. Computed Depositions

285

286 The results of the computer modelling of the transport by air of nitrogen oxides and ammonia
 287 from their sources to the coastal waters in the 2Seas region are presented here. The computer
 288 model uses weather data and emissions data to calculate the transport and deposition of these
 289 nitrogen containing gases. The examples provided are for emissions in 2000 and 2009 and
 290 historical weather data for 2009 and 2011. All four combinations between these emission and

291 simulation years are included, so that comparisons can be made and the effect of both the
 292 emissions and the weather can be demonstrated. As mentioned previously, only sources in the
 293 ISECA chosen window (-6 to 7°E, 48 to 54°N) are included in the simulations - to highlight
 294 the local contribution to local eutrophication. In Figures 5 and 7 total annual deposited
 295 quantities are shown for nitrogen oxides and ammonia. Figure 6 presents the 2009 NO_x
 296 deposits which are only due to shipping and other mobile machinery, excluding road
 297 transport (SNAP sector 8).
 298

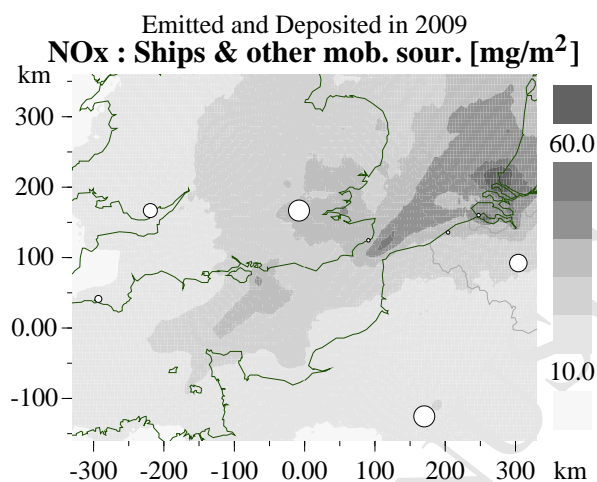


Figure 6. Modelled 2009 nitrogen oxides deposits from shipping and other (non-road) mobile emitters (SNAP sector 8)

299

300 7. Analysis and Discussion

301

302 The significantly higher NO_x emissions in 2000 compared to 2009 (Figure 3) result in visible
 303 increase in the computed depositions in Figure 5, while for ammonia the difference in both
 304 emissions and depositions (Figure 7) is much smaller. However, the deposited amounts of
 305 ammonia are 7.5 times higher than the corresponding NO_x depositions. This can be
 306 explained with the fact that ammonia is a hydrophilic compound, i.e. the Henry's law
 307 constant (FLEXPART, 2014) for ammonia is many times higher than the corresponding one
 308 for nitrogen oxides.

309

310 In Figure 6, showing the deposition map for SNAP sector 8, the busiest shipping routes
 311 through the narrow Strait of Dover as well as the seaborne traffic surrounding the port areas
 312 of Antwerp and Rotterdam dominate deposition and become visible on the contour plot. The
 313 high deposition rate is due first to the fact that shipping is the main pollutant within SNAP
 314 sector 8 and, second, as the smoke of the ships engines is dragged by the ship's wake over the
 315 sea surface, it has greater chance to react with the water directly while inland emissions
 316 undergo a longer cycle of transport to the clouds and deposition with the rain.

317

318 The influence of the weather on the atmospheric deposition of nitrogen nutrients can be seen
 319 by comparing the left and right halves of Figures 5 and 7: 2011 was drier than 2009
 320 (illustrated in Figure 8 showing actual recorded rainfall in three UK locations) which results
 321 in lower deposits, especially of NO_x. Most pronounced are the differences in nitrogen oxides
 322 depositions over England where the 2011 quantities are on average with 20 mg/m² lower than
 323 in 2009. The quantities emitted within the model domain but not deposited there are
 324 transported by the wind across the domain boundaries.

325

326 The model set-up is operational; new meteorological data can be freely downloaded and
 327 further simulations can be done with either free or proprietary emissions data as needed. It is
 328 quite possible to run the model with emissions data available from previous years (e.g. from
 329 EMEP) and with current meteorological data – in this way estimates can be made of the
 330 atmospheric input (e.g. during the winter months) which can help predict the occurrence of
 331 potentially harmful algal blooms in the spring.
 332

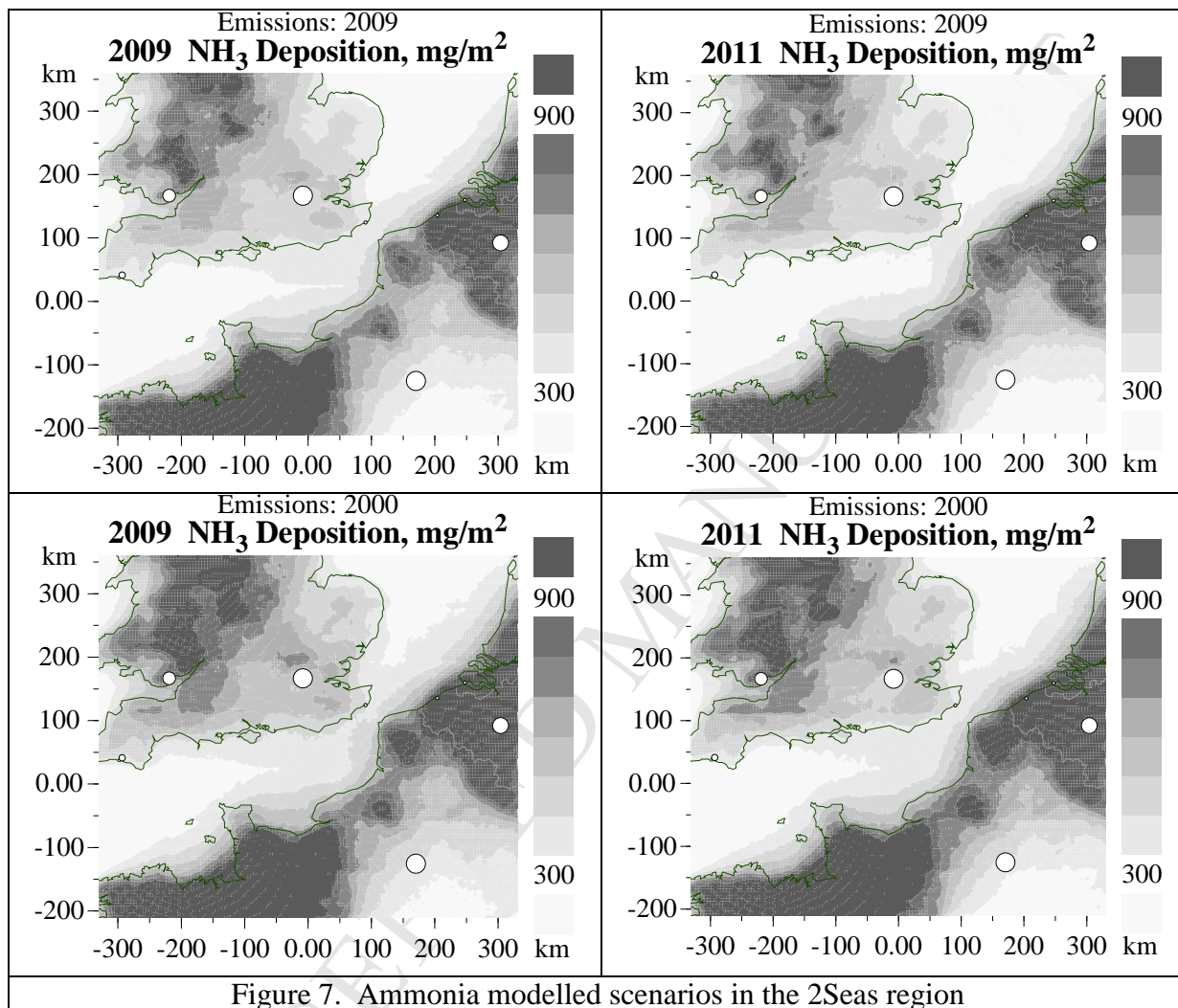


Figure 7. Ammonia modelled scenarios in the 2Seas region

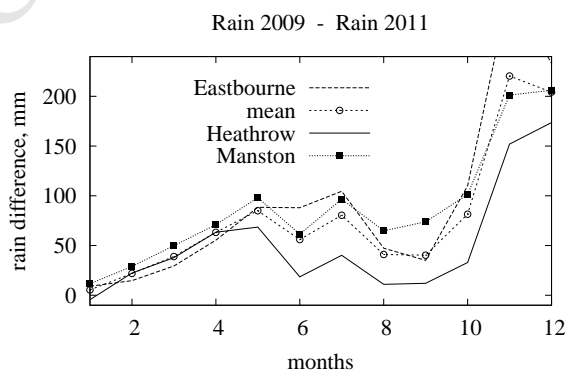


Figure 8. Difference in monthly rainfall over south-east England between 2009 and 2011, source: (Met Office, 2014)

334 The simulation results can be used in a number of ways to highlight various aspects of the
335 problem of coastal waters eutrophication: The combined contribution all SNAP sectors from
336 the sources in the chosen region can be displayed graphically (as in Figures 5, 7) or
337 numerically for the areas of interest. The effect of any of the SNAP sectors can be traced
338 individually (as in Figure 6). The emitted quantities which have not been deposited within
339 the target domain but are transported through its boundaries are recorded over the duration of
340 the simulation and can be analysed. The effect of the weather can be investigated by running
341 the same emissions with meteorological data from two or more different years (as in Figures
342 5 and 7).

343
344 The presented results show that, of all seas in the investigated region, the coastal areas of
345 Belgium and the Netherlands receive the highest depositions of both NO_x and ammonia.
346 These atmospheric deposits are in addition to the riverine inputs as shown by other models
347 (Vermaat, 2012; Shutler, 2011; Lacroix, 2007). Those models, backed by satellite
348 observations, indicate the waters near the continental coast (French, Belgian and Dutch) of
349 the eastern English Channel and the southern North Sea as usually having the highest
350 concentrations of chlorophyll-*a* which means those are the zones with the most severe
351 eutrophication in the 2Seas region. So the atmospheric depositions contribute to making that
352 eutrophication even worse.

353
354 Further improvement of the model is possible in the following ways. The meteorological
355 time-step can be reduced from 6 hours to the recommended 3 hours (Stohl, 2005). In the
356 ERA-Interim dataset (ECMWF, 2014), 3-hourly records are available as short-term (12-hour)
357 forecasts run twice daily. Although this shorter time-step is more appropriate for tracing
358 single pollution events, the enhanced accuracy may be useful for estimating the atmospheric
359 input of nutrients to the sea water in the days and weeks immediately preceding an algal
360 bloom (e.g. in April; Lacroix, 2007). Around critical emitting areas, e.g. Brittany in France
361 where significant quantities of ammonia is released by agriculture (Figure 2, right), it may be
362 appropriate to refine the resolution of the weather information with the help of a numerical
363 weather prediction package (WRF, 2014). In such a way the tendency of ammonia to be
364 deposited nearer to the source will be better resolved and the estimate of this route of
365 eutrophication of the surrounding seas will become more accurate. In one or two years, when
366 emissions data with the improved spatial resolution of 0.1 degrees become freely available
367 (CEIP, 2015), the model can be adjusted to provide better estimates (with or without WRF
368 weather refinement) of the local polluters' contribution to the local eutrophication in selected
369 regions. Then comparisons can be made with the trans-boundary pollution calculated and
370 reported by EMEP thus helping local policy decisions.

371 372 **8. Conclusions**

373
374 A model of the atmospheric transport of pollutants responsible for eutrophication has been
375 constructed, which couples the effects of pollution emitting sources within the area of
376 interest, with weather dynamics. A Lagrangian Particle Dispersion approach is used (the code
377 FLEXPART) to model atmospheric transport and deposition. With emissions databases
378 which contain information about the types of pollutant sources (e.g. SNAP sectors) the model
379 can distinguish between the various emission sources highlighting their contribution to the
380 deposited quantities. In this way the effect of different industrial sectors and agriculture on
381 airborne eutrophication can be estimated. A discretisation that employs coarse-grid weather
382 data and fine-grid emissions data shows that: (a) Ammonia is responsible for the largest share
383 of nitrogen deposits from the atmosphere. This can be explained with the fact that, being

384 more soluble, ammonia is deposited more easily and nearer the sources. Overall, agriculture
385 contributes more (in the form of ammonia) than all the local NO_x sources. (b) In contrast,
386 nitrogen oxide emissions are more likely to leave the region and be deposited elsewhere.
387 (Far-away emissions which may be carried by the wind and be deposited in the 2Seas region
388 are not part of these simulations.) (c) Heavy nutrient load from the atmosphere to the coastal
389 waters of Belgium and the Netherlands is observed in the considered model scenarios.

390

391 When used with near real-time weather data (freely available from ECMWF) the presented
392 model can, in conjunction with other models for the riverine input of nutrients, be used to
393 forecast algal blooms in the eastern English Channel and the southern North Sea.
394 Alternatively, retrospective calculations with historical weather records can help analyse and
395 understand the mechanisms and evolution of the atmospheric part of the eutrophication
396 phenomenon.

397

398

399 **Acknowledgments**

400

401 This work forms part of the project ISECA, Part-financed by ERDF through the Interreg IV
402 A 2-Seas Programme “Investing in your Future”

403

404

405 **References**

406

407 AirBase (2014): <http://acm.eionet.europa.eu/databases/airbase>

408

409 Anderson, D.M., Glibert, P.M., Burkholder, J.M. (2002): Harmful algal blooms and
410 eutrophication: Nutrient sources, composition, and consequences. *Estuaries* **25** (4), 704-726.

411

412 Boynton, W. R., Kemp, W. M. & Keefe, C. W. (1982): A comparative analysis of nutrients
413 and other factors influencing estuarine phytoplankton production. In *Estuarine comparisons*
414 (Kennedy, V. S., ed.). Academic Press, New York, pp. 69–90.

415

416 CEIP (2015): http://www.ceip.at/ms/ceip_home1/ceip_home/new_emep-grid/

417

418 ECMWF (2014): The European Centre for Medium-Range Weather Forecasts:

419 http://data-portal.ecmwf.int/data/d/interim_full_daily/levtype=ml/

420 <http://www.ecmwf.int/en/research/climate-reanalysis/era-interim>

421

422 EMEP (2014): The European Monitoring and Evaluation Programme.

423 http://www.emep.int/mscw/Grid/emep_grid.html

424

425 FLEXPART (2014): <http://flexpart.eu>

426

427 Hecky, R. E. and Kilham, P. (1988): Nutrient limitation of phytoplankton in freshwater and
428 marine environments: A review of recent evidence on the effects of enrichment. *Limnology*
429 *and Oceanography* **33** (4), 796–822.

430

431 INTERREG (2014): <http://www.interreg4a-2mers.eu/programme/en>

432

- 433 Information System on the Eutrophication of our Coastal Waters, ISECA (2014):
434 <http://www.iseca.eu/en/>
435
- 436 KentAir (2014): <http://www.kentair.org.uk/data/data-selector>
437
- 438 Lacroix, G., Ruddick, K., Park, Y., Gypens, N., Lancelot, C. (2007): Validation of the 3D
439 biogeochemical model MIRO&CO with field nutrient and phytoplankton data and MERIS-
440 derived surface chlorophyll-a images. *Journal of Marine Systems* **64**, 66–88.
- 441 Ly, Juliette; Catharina J.M. Philippart, Jacco C. Kromkamp (2014): Phosphorus limitation
442 during a phytoplankton spring bloom in the western Dutch Wadden Sea, *Journal of Sea*
443 *Research* **88**, 109-120.
444
- 445 Maes, Joachim; Jo Vliegen, Karen Van de Vel, Stijn Janssen, Felix Deutsch, Koen De
446 Ridder (2009): Spatial surrogates for the disaggregation of CORINAIR emission inventories.
447 *Atmospheric Environment*, **43**, 1246-1254.
448
- 449 Met Office (2014): <http://www.metoffice.gov.uk/public/weather/climate-historic/>
450
- 451 NCEP (2014): <http://rda.ucar.edu/datasets/ds083.2/>
452
- 453 Nedwell, D. B.; L. F. Dong, A. Sage and G. J. C. Underwood (2002): Variations of the
454 Nutrients Loads to the Mainland U.K. Estuaries: Correlation with Catchment Areas,
455 Urbanization and Coastal Eutrophication, *Estuarine, Coastal and Shelf Science* **54**, 951–970.
456
- 457 OSPAR (2013): “Distance to target” modelling assessment. www.ospar.org
458
- 459 Paerl, Hans W. (1997): Coastal eutrophication and harmful algal blooms: Importance of
460 atmospheric deposition and groundwater as “new” nitrogen and other nutrient sources,
461 *Limnol. Oceanogr.* **42** (5, part 2), 1154-1165.
462
- 463 Peierls, B. L., Caraco, N. F., Pace, M. L. & Cole, J. J. (1991): Human influence on river
464 nitrogen. *Nature* **350**, 386–387.
465
- 466 Plainiotis, S., Pericleous, K.A., Fisher, B.E.A. and Shieri, L. (2010): Application
467 of Lagrangian particle dispersion models to air quality assessment in the Trans-Manche
468 region of Nord-Pas-de-Calais (France) and Kent (Great Britain), *Int. J. Environment and*
469 *Pollution*, Vol. **40**, Nos. 1/2/3, pp.160–174.
470
- 471 Plainiotis, S., Pericleous, K.A., Fisher, B.E.A. and Shier, L. (2005a): Forward and inverse
472 transport of particulate matter and gaseous pollutants affecting the region bordering the
473 English Channel, Proceedings of the 16th IASTED International Conference on Modelling
474 and Simulation (MS-2005), Acta Press 459–090, pp.164–169.
475
- 476 Plainiotis, S., Pericleous, K.A., Fisher, B.E.A. and Shier, L. (2005b): Modelling high
477 particulate matter and ozone episodes in the trans-Manche region, Abstracts of the 5th
478 International Conference on Urban Air Quality, p.89.
479
- 480 Shutler, J.D., T.J. Smyth, S. Saux-Picart, S.L. Wakelin, P. Hyder, P. Orekhov, M.G. Grant,
481 G.H. Tilstone, J.I. Allen (2011): Evaluating the ability of a hydrodynamic ecosystem model

- 482 to capture inter- and intra-annual spatial characteristics of chlorophyll-a in the north east
483 Atlantic, *Journal of Marine Systems* **88**, 169–182.
- 484
- 485 SNAP (2014): www.emep.int/UniDoc/node7.html
- 486
- 487 Spokes, Lucinda J. and Tim D. Jickells (2005): Is the atmosphere really an important source
488 of reactive nitrogen to coastal waters? *Continental Shelf Research* **25**, 2022–2035.
- 489
- 490 Stohl, A.; Hittenberger, M. and Wotawa, G. (1998): Validation of the Lagrangian particle
491 dispersion model FLEXPART against large-scale tracer experiment data. *Atmos. Environ.*,
492 **32**, 4245–4264.
- 493
- 494 Stohl, A.; C. Forster, A. Frank, P. Seibert, and G. Wotawa (2005): Technical Note : The
495 Lagrangian particle dispersion model FLEXPART version 6.2. *Atmos. Chem. Phys.* **5**, 2461-
496 2474; <http://flexpart.eu>
- 497
- 498 Thomson, D. J. (1987): Criteria for the selection of stochastic models of particle trajectories
499 in turbulent flows. *J. Fluid Mech.*, **180**, 529–556.
- 500
- 501 Thunis, P., A. Pederzoli, D. Pernigotti (2012): Performance criteria to evaluate air quality
502 modeling applications. *Atmospheric Environment* **59** (2012), 476–482.
- 503
- 504 Troost, T.A.; M. Blaas, F.J. Los (2013): The role of atmospheric deposition in the
505 eutrophication of the North Sea: A model analysis, *Journal of Marine Systems* **125**, 101-112.
- 506
- 507 Uliasz, M. (1994): Lagrangian particle dispersion modeling in mesoscale applications. In:
508 Zannetti, P. (ed.): *Environmental Modeling*, Vol. II. Computational Mechanics Publications,
509 Southampton, UK.
- 510
- 511 Vermaat, J.E., Broekx, S., Van Eck, B., Engelen, G., Hellmann, F., De Kok, J.L., Van der
512 Kwast, H., Maes, J., Salomons, W. and Van Deursen, W. (2012): Nitrogen source
513 apportionment for the catchment, estuary and adjacent coastal waters of the Scheldt, Special
514 Issue - A Systems Approach for Sustainable Development in Coastal Zones, *Ecology and*
515 *Society* **17** (2): 30.
- 516
- 517 WebDab (2014): http://www.ceip.at/ms/ceip_home1/ceip_home/webdab_emepdatabase/
- 518
- 519 WRF model (2014): <http://www2.mmm.ucar.edu/wrf/users/>
- 520
- 521 WRI (2014): [http://www.wri.org/our-work/project/eutrophication-and-hypoxia/sources-](http://www.wri.org/our-work/project/eutrophication-and-hypoxia/sources-eutrophication)
522 [eutrophication](http://www.wri.org/our-work/project/eutrophication-and-hypoxia/sources-eutrophication)
- 523
- 524 Zoua, L.; H.T. Chena, J. Zhanga (2000): Experimental examination of the effects of
525 atmospheric wet deposition on primary production in the Yellow Sea, *Journal of*
526 *Experimental Marine Biology and Ecology* **249**, 111–121.
- 527

Weather data, emissions data and Lagrangian computations form the numerical model.

Deposition maps in a target geographical region are produced and compared.

Individual polluting industrial or transport sectors can be traced.

Atmospheric deposition of nitrogen eutrophicants increases in wet weather.

Heaviest atmospheric deposition adds to high riverine input in some coastal regions.